A fundamental role of mAbp1 in neutrophils: impact on β_2 integrin–mediated phagocytosis and adhesion in vivo

*Jürgen Schymeinsky,[1] *Ronald Gerstl,[1] Ingrid Mannigel,[1] Katy Niedung,[1] David Frommhold,[2] Klaus Panthel,[3] Jürgen Heesemann,[3] Michael Sixt,[4] Thomas Quast,[5] Waldemar Kolanus,[5] Attila Mocsai,[6] Jürgen Wienands,[7] Markus Sperandio,[1] and Barbara Walzog[1]

[1]Walter Brendel Centre for Experimental Medicine, Ludwig-Maximilians-University Munich, Munich, Germany; [2]Department of Neonatology, Children's Hospital, University of Heidelberg, Heidelberg, Germany; [3]Max von Pettenkofer-Institute for Hygiene and Medical Microbiology, Ludwig-Maximilians-University Munich, Munich, Germany; [4]Department of Molecular Medicine, Max Planck Institute of Biochemistry, Martinsried, Germany; [5]LIMES Institute (Life and Medical Sciences Bonn) Program Unit Molecular Immune and Cell Biology, Laboratory of Molecular Immunology, University of Bonn, Bonn, Germany; [6]Department of Physiology, Semmelweis University School of Medicine, Budapest, Hungary; and [7]Institute of Cellular and Molecular Immunology, Georg-August-University of Göttingen, Göttingen, Germany

The mammalian actin-binding protein 1 (mAbp1, Hip-55, SH3P7) is phosphorylated by the nonreceptor tyrosine kinase Syk that has a fundamental effect for several β_2 integrin (CD11/CD18)–mediated neutrophil functions. Live cell imaging showed a dynamic enrichment of enhanced green fluorescence protein–tagged mAbp1 at the phagocytic cup of neutrophil-like differentiated HL-60 cells during β_2 integrin–mediated phagocytosis of serum-opsonized *Escherichia coli*. The genetic absence of Syk or its pharmacologic inhibition using piceatannol abrogated the proper localization of mAbp1 at the phagocytic cup. The genetic absence or down-regulation of mAbp1 using the RNA interference technique significantly compromised β_2 integrin–mediated phagocytosis of serum-opsonized *E coli* or *Salmonella typhimurium* in vitro as well as clearance of *S typhimurium* infection in vivo. Moreover, the genetic absence of mAbp1 almost completely abrogated firm neutrophil adhesion under physiologic shear stress conditions in vitro as well as leukocyte adhesion and extravasation in inflamed cremaster muscle venules of mice treated with tumor-necrosis factor α. Functional analysis showed that the down-regulation of mAbp1 diminished the number of β_2 integrin clusters in the high-affinity conformation under flow conditions. These unanticipated results define mAbp1 as a novel molecular player in integrin biology that is critical for phagocytosis and firm neutrophil adhesion under flow conditions. (Blood. 2009;114:4209-4220)

Introduction

The mammalian actin-binding protein 1 (mAbp1, drebrin-like protein, SH3P7, HIP-55) is an adaptor protein that is characterized by a well-defined actin-binding module, the actin-depolymerizing factor homology domain.[1,2] The 55-kDa protein mAbp1 is expressed in a wide variety of murine tissues and contains a single actin-depolymerizing factor homology domain at its N-terminal side followed by a helical domain that are both required for efficient actin binding.[2] At its C-terminal end, mAbp1 contains a Src homology 3 domain and a proline-rich domain that is known to be phosphorylated by Src- and Syk-family kinases in leukocytes and in the human breast cancer cell line MCF-7.[1,3,4] The yeast Abp1 homologue (Abp1p) contains 2 acidic domains that interact with the actin-related protein (Arp) 2/3 complex, thereby recruiting it to actin filaments.[5] The Arp 2/3 complex is required for the initiation of actin polymerization, a process that is regulated by nucleation promoting factors (NPFs), such as Abp1p in yeast. The mammalian mAbp1 protein does not contain an equivalent acidic domain, and it bears no NPF activity.[2] In neuronal cells, mAbp1 has been shown to exert its regulatory effect on actin dynamics indirectly by interacting with the neuronal Wiskott-Aldrich syndrome protein (N-WASP), a member of the WASP family proteins that act as NPFs.[6]

Several studies have linked the Abp1p/mAbp1 function to receptor-mediated endocytosis and vesicle trafficking in yeast and mammalian cells.[5,7] The mAbp1$^{-/-}$ mice suffer from splenomegaly, hypertrophy of the heart, lung edema, and behavioral abnormalities.[8,9] Less is known about the effect of mAbp1 for leukocyte functions. However, defective T-cell receptor–mediated signaling has been shown in mAbp1$^{-/-}$ T cells.[9] In mAbp1$^{-/-}$ B cells, impaired antigen processing and presentation caused by reduced antigen internalization was reported.[10]

Adhesion molecules of the β_2 integrin (CD11/CD18) family play a pivotal role in the recruitment of polymorphonuclear neutrophils (PMNs) to sites of inflammation by mediating, eg, slow leukocyte rolling, firm adhesion, adhesion strengthening, and intraluminal crawling of PMNs.[11] On ligand binding, β_2 integrins induce profound tyrosine signaling, including activation of the nonreceptor tyrosine kinase Syk.[12-14] Similar to immunoreceptor signaling, Syk activation by β_2 integrins involves the immunoreceptor tyrosine-based activation motif–bearing adaptor proteins DAP12 and the Fc receptor (FcR) γ-chain that are phosphorylated by Src-family kinases.[15] Syk controls different β_2 integrin–mediated PMN functions, including slow leukocyte rolling and firm adhesion during inflammation in vivo, as well as the respiratory burst, cell

Submitted February 18, 2009; accepted July 13, 2009. Prepublished online as *Blood* First Edition paper, July 28, 2009; DOI 10.1182/blood-2009-02-206169.

*J.S. and R.G. contributed equally to this study

The online version of this article contains a data supplement.

The publication costs of this article were defrayed in part by page charge payment. Therefore, and solely to indicate this fact, this article is hereby marked "advertisement" in accordance with 18 USC section 1734.

spreading, migration, and phagocytosis.[16-20] Because Syk has been reported to phosphorylate mAbp1 in leukocytes,[1] β_2 integrin–mediated PMN functions such as phagocytosis and adhesion may also involve mAbp1. However, this hypothesis has not been addressed to date.

In this study, we identified mAbp1 as a new molecular player in PMN biology. The absence or down-regulation of mAbp1 induced a severe defect in β_2 integrin–mediated engulfment of serum-opsonized *Escherichia coli* or *Salmonella enterica subsp enterica serovar typhimurium* (*S typhimurium*), showing a fundamental role of mAbp1 for phagocytosis. This unexpected role of mAbp1 was confirmed by imaging the spatiotemporal dynamics of mAbp1 enrichment at the phagocytic cup. The relevance of mAbp1 for innate control of bacterial infection was shown in mAbp1$^{-/-}$ mice that were orally infected with *S typhimurium*. Moreover, mAbp1 was indispensable for PMN adhesion in TNFα-stimulated cremaster muscle venules and in a flow chamber under shear stress conditions, indicating an additional role of mAbp1 for PMN adhesion under flow conditions. The adhesion defect was associated with a reduced number of CD18 clusters in the high-affinity conformation, suggesting an effect of mAbp1 on the reinforcement of the high-affinity conformation of the β_2 integrins under flow conditions. Thus, mAbp1 seems to be of fundamental importance for different PMN functions both in vitro and in vivo.

Methods

Plasmids, antibodies, and reagents

The mAbp1-EGFP cDNA was a generous gift of Dr Marcel Deckert (Université de Nice Sophia Antipolis, Nice, France).[21] For further information on reagents, the generation of the lentiviral vectors, and the stable HL-60 cell lines, please see supplemental Methods (available on the *Blood* website; see the Supplemental Materials link at the top of the online article).

Mice

Mice carrying the Syk^{tm1Tyb} allele (referred to as Syk^{-}) were maintained as Syk$^{+/-}$ heterozygotes on the C57BL/6 genetic background.[22] The generation of mice with a Syk$^{-/-}$ hematopoietic system was performed as described previously.[17] Mice carrying the Dbnl^{tm1Jwnd} allele (mAbp1^{-}) were maintained on the BALB/c background.[8] Rag1^{tm1Mom} (Rag1^{-}) mice[23] were purchased from Jaxmice (The Jackson Laboratory). Mice carrying the Itgb2$^{tm1Bay/J}$ (CD18^{-}) allele[24] were kindly provided by K. Scharffetter-Kochanek (University of Ulm, Ulm, Germany). Animal experiments were approved by all participating institutions.

Isolation of bone marrow PMNs and cell culture

Murine PMNs were isolated as described previously[25] and analyzed by flow cytometry as described in supplemental Methods. Cell culture, neutrophil-like differentiation of HL-60 cells, and pharmacologic inhibition of Syk were performed as described.[25]

PMN adhesion and phagocytosis in vitro

Adhesion of murine PMNs (10^5/well) was analyzed in triplicates in 96-well microtiter plates coated with murine fibrinogen (50 μg/mL) as described previously.[16] Detailed description of adhesion experiments under flow conditions is provided in supplemental Methods. For the analysis of phagocytosis, fluorescein isothiocyanate–conjugated *E coli* particles (Invitrogen) and the invasion-deficient (ΔinvG)[26] *S typhimurium* strain SB161 were opsonized with human serum, heat-inactivated murine serum, or native murine serum for 30 minutes at 37°C. Opsonized *E coli* bacteria and dHL-60 cells or murine PMNs in RPMI 1640 (3×10^6 cells/mL) were incubated at a bacteria-to-cell ratio of 100:1 for indicated times at 37°C. Phagocytosis was stopped by ice-cold 3.7% formaldehyde for 30 minutes. For quantitative analysis, cells were resuspended in 1.25 mg/mL trypan blue to quench extracellular signals, and images were captured using a 20×/0.75 numeric aperture (NA) objective and a Zeiss Axiovert 200M microscope. Phagocytosis was scored off-line in a blinded manner, and cells that engulfed at least one *E coli* were defined as positive. To assess phagocytosis of serum-opsonized SB161 bacteria, PMNs were plated on 24-well plates (10^5/well) and incubated with a bacteria-to-cell ratio of 10:1 for 15 minutes at 37°C. To kill extracellular bacteria, gentamycin (100 μg/mL) was added to the medium for 30 minutes at 37°C. Subsequently, PMNs were washed twice with PBS and lysed with 1% Triton X-100 in PBS, and bacteria were plated in appropriate dilutions in triplicate on LB-agar plates to determine the number of colony-forming units (CFUs).

Infection of mice with the *S typhimurium* wild-type strain SL1344

Mice were orogastrically infected by round-bottomed gavages with a single dose of 5×10^7 CFU of *S typhimurium* wild-type strain SL1344.[27] Two days after infection, mice spleens were removed, weighed, and homogenized in PBS supplemented with 0.25% Tween 20 (Sigma-Aldrich). CFUs were determined in duplicate by plating appropriate dilutions on LB-agar plates.

Scanning and spinning disc confocal microscopy

Indirect immunostaining was performed as described.[25] Confocal scanning microscopy of fixed cells was conducted with a Zeiss LSM 410/Axiovert 135 microscope with a Zeiss 63×/1.2 NA water or a Zeiss 63×/1.4 NA oil objective. Confocal microscopy of live mAbp1-EGFP cells phagocytosing opsonized Alexa 594–labeled *E coli* was performed with an Olympus Fluoview 1000 confocal microscope equipped with a Plapo 60×/1.4 NA oil-immersion objective (Olympus) and a climate chamber (37°C/5% CO_2, humidity). Three-dimensional (3D) projections were generated with Olympus Fluoview software and Imaris software (Bitplane). Confocal spinning disc microscopy was performed with a Zeiss αPlan-Fluar 100×/1.45 NA oil objective on a Zeiss Axiovert 200M microscope with a CSU10 spinning disc scanhead (Yokogawa), Coolsnap HQ2 camera (Roper Scientific), run by Metamorph software (Molecular Devices). The system was implemented by Visitron Systems.

Intravital microscopy

Intravital microscopy and recording of the cremaster muscle was conducted as reported previously.[28] Microvascular parameters were measured with a digital image-processing system.[29] The number of adherent leukocytes in inflamed cremaster muscle venules was assessed as described.[28] Leukocytes were considered to be adherent when they were attached at the same position for more than 30 seconds. To quantify intravascular and extravascular leukocytes, cremaster muscle whole mounts were prepared as reported.[25] Detailed description of the (autoperfused) microflow chamber model is provided as supplemental Methods.

Statistical analysis

Statistical significance was determined with the Student *t* test, the Mann-Whitney rank sum test, or the Kruskal-Wallis ANOVA test, respectively. Data shown represent means plus or minus SDs or plus or minus SEMs. Values of *P* less than .05 were considered statistically significant.

Results

Fundamental role of mAbp1 for phagocytosis and bacterial clearance in vivo

Phagocytosis is a sequential process that involves particle recognition, actin-dependent particle uptake, and phagosome closure.[30] To study the functional effect of mAbp1 for β_2 integrin–mediated

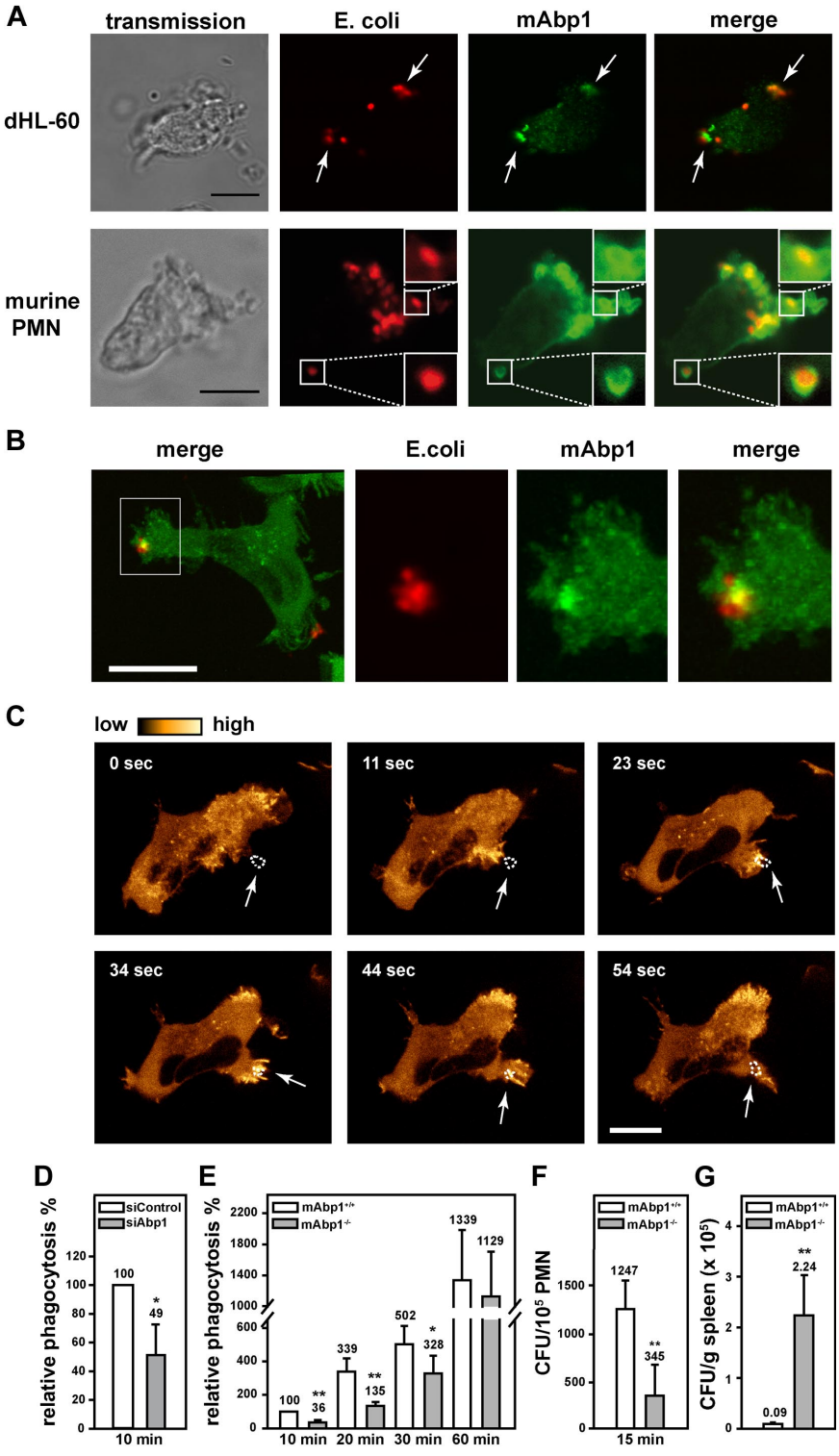

Figure 1. A fundamental role of mAbp1 for phagocytosis and bacterial clearance in vivo. (A) Confocal microscopy images of dHL-60 cells and murine PMNs phagocytosing serum-opsonized Alexa 594–conjugated *E coli* (red). mAbp1 (green) was enriched at the site of particle binding (arrows). Bar = 10 μm. (B) Maximal 3D projection of confocal images taken with an interval of 0.4 μm of a dHL-60 cell expressing mAbp1-EGFP (green) phagocytosing Alexa 594–labeled *E coli* (red). Please see supplemental Figure 1 and supplemental Video 1 for three-dimensional (3D) animation. Bar = 5 μm. (C) Confocal spinning disc microscopy of a dHL-60 cell expressing mAbp1-EGFP during phagocytosis of serum-opsonized Alexa 594–conjugated *E coli*. Consecutive images at indicated time points were extracted from the original recording that was performed with a frame rate of 1 picture per second (please see supplemental Video 2). For better visualization, the EGFP fluorescence intensity was processed to pseudocolors. mAbp1 was dynamically enriched at the binding site (arrows) of the *E coli* particle (dotted line). Bar = 10 μm. Phagocytosis of serum-opsonized *E coli* particles by (D) siAbp1 dHL-60 cells or (E) murine mAbp1$^{-/-}$ PMNs compared with siControl (100%) or mAbp1$^{+/+}$ PMNs (100%). (D-E) Mean relative phagocytosis ± SD; n = 4. (F) Phagocytosis of serum-opsonized *S typhimurium* invasion-deficient strain SB161 by murine mAbp1$^{-/-}$ and mAbp1$^{+/+}$ PMNs. Mean number of CFU per 10^5 PMN; n = 3. (G) Bacterial load of spleens of mAbp1$^{+/+}$ and mAbp1$^{-/-}$ mice 48 hours after oral infection with 5×10^7 CFU of *S typhimurium* wild-type strain SL1344. Mean CFU $\times 10^5$/g spleen ± SEM; n = 4; **P* < .05; ***P* < .005.

phagocytosis, we analyzed the subcellular localization of mAbp1 during engulfment of serum-opsonized *E coli* in dHL-60 cells and in murine PMNs. In this model, phagocytosis is mediated by the complement protein iC3b that is recognized by the macrophage adhesion molecule-1 (Mac-1), a member of the β_2 integrin family consisting of the β_2 integrin chain (CD18) and the α_M integrin chain (CD11b).[30] By means of confocal microscopy, mAbp1 was found to be markedly enriched at the site of particle binding in dHL-60 cells and in native murine PMNs as shown by antibody staining of mAbp1 (Figure 1A). To delineate the spatial and temporal dynamics of the translocation of mAbp1 during phagocytosis, its subcellular localization was studied by live cell imaging in a dHL-60 cell clone that homogenously expressed EGFP-tagged mAbp1 (mAbp1-EGFP) at a level comparable with wild-type mAbp1 (supplemental Figure 1A-B). The recording of z-stacks of phagocytosing mAbp1-EGFP dHL-60 cells with a scanning confocal microscope followed by off-line processing of the images to generate 3D animations and maximal 3D projections verified the translocation of mAbp1 to the particle binding site with high 3D resolution (Figure 1B; supplemental Figure 2; supplemental

Video 1). The analysis of mAbp1 dynamics with high temporal resolution with confocal spinning disc microscopy showed that mAbp1-EGFP was transiently enriched at the forming phagocytic cup within seconds and disappeared on particle engulfment (Figure 1C; supplemental Video 2). To study the functional relevance of these findings, stable HL-60 cell clones were generated in which mAbp1 expression was down-regulated by the RNA interference (RNAi) technique (supplemental Figure 3). Phagocytosis of serum-opsonized *E coli* particles was significantly impaired in siAbp1 dHL-60 cells after 10 minutes compared with control cells (100%) at the same time point (cells that engulfed at least one *E coli* particle were defined as positive, and extracellular signals were quenched by trypan blue; Figure 1D). This result was confirmed in PMNs from mAbp1$^{-/-}$ mice in which phagocytosis was significantly compromised within 10 minutes, 20 minutes, and 30 minutes after the onset of the experiment compared with mAbp1$^{+/+}$ PMNs (Figure 1E). Further analysis showed that the percentage of mAbp1$^{+/+}$ PMNs that engulfed more than one bacterium was significantly higher than that observed in mAbp1$^{-/-}$ PMNs (60.9% ± 13.2% vs 40.1% ± 12.8%; 20 minutes; n = 3; $P < .05$). After 60 minutes, phagocytosis of mAbp1$^{-/-}$ PMNs was similar to the levels observed in mAbp1$^{+/+}$ PMNs, indicating that mAbp1 was only critical for the efficient particle engulfment at early time points. Because the efficiency of phagocytosis is decisive to overcome bacterial infection, we studied the relevance of mAbp1 for phagocytosis of pathogens with the use of the invasion-deficient *S typhimurium* strain SB161 (referred to as SB161). Because of the absence of the type III secretion system 1 in this strain, bacteria uptake strictly depends on the phagocytic capacity of the PMNs.[31] Phagocytosis of serum-opsonized SB161 was found to be dramatically compromised after 15 minutes in mAbp1$^{-/-}$ PMNs (Figure 1F). Moreover, phagocytosis was almost completely absent without serum opsonization of SB161, indicating that engulfment of *S typhimurium* was strictly dependent on β_2 integrins (data not shown). To study the effect of mAbp1 for clearance of bacterial infection in vivo, we orally administered a lethal dose of 5×10^7 CFU of the wild-type strain of *S typhimurium* (SL1344) to mAbp1$^{+/+}$ and mAbp1$^{-/-}$ mice. Within 48 hours after infection, the bacterial load was significantly higher in the spleen of mAbp1$^{-/-}$ mice compared with spleen of Abp1$^{+/+}$ mice, indicating a role of mAbp1 for innate control of bacterial infection in vivo (Figure 1G).

Effects were specific for mAbp1 and independent of FcγR engagement

To study the specificity of the observed phagocytosis defect, the expression of Mac-1 (CD11b/CD18) and the PMN differentiation marker GR-1 on the cell surface of mAbp1$^{-/-}$ and mAbp1$^{+/+}$ PMNs was determined by flow cytometry (Figure 2A). The expression of all 3 surface antigens was unaffected in the absence of mAbp1, indicating that the observed phagocytosis defect was not due to incomplete PMN differentiation or compromised CD11b/CD18 expression. Similarly, the up-regulation of CD11b/CD18 expression on the cell surface on stimulation with keratinocyte-derived chemokine (KC, CXCL1) or TNFα for 30 minutes was almost identical to the response obtained from mAbp1$^{+/+}$ control PMNs, showing that the mobilization of CD11b/CD18 from intracellular stores in specific granules and secretory vesicles to the cell membrane was normal. Moreover, confocal microscopy showed that particle binding as well as CD18 clustering were still intact in the absence of mAbp1 (Figure 2B). To test whether mAbp1 was required for integrin activation, we measured the binding of Alexa 488–conjugated fibrinogen to Mn^{2+}- or TNFα-stimulated PMNs obtained from mAbp1$^{+/+}$ or mAbp1$^{-/-}$ mice (Figure 2C). On stimulation with Mn^{2+} (3 mM) or TNFα (100 ng/mL), fibrinogen binding to mAbp1$^{+/+}$ PMNs was significantly enhanced compared with unstimulated control cells or EDTA-treated negative control. Similar results were obtained with mAbp1$^{-/-}$ PMNs, indicating that mAbp1 was not required for activation of the β_2 integrin Mac-1 that acts as receptor for fibrinogen on PMNs. To confirm that phagocytosis of serum-opsonized *E coli* in the used assay strictly depended on engagement of Mac-1, phagocytosis was studied with CD18$^{-/-}$ and CD18$^{+/+}$ PMNs (supplemental Figure 4A). As expected, CD18$^{+/+}$ PMNs performed substantial phagocytosis that was almost completely absent in CD18$^{-/-}$ PMNs. The proinflammatory cytokine TNFα is known to stimulate phagocytosis of leukocytes,[30] but it was unable to rescue phagocytosis in CD18$^{-/-}$ PMNs. To further confirm that complement-mediated phagocytosis depended on Mac-1 in our assay, we measured the uptake of *E coli* particles after incubation with heat-inactivated serum (supplemental Figure 4B). In mAbp1$^{-/-}$ and mAbp1$^{+/+}$ PMNs, particle uptake was significantly reduced compared with opsonization with native serum (100%), confirming that phagocytosis depended on Mac-1. To exclude a putative involvement of FcγR-mediated signaling during complement-mediated phagocytosis, particle engulfment of mAbp1$^{-/-}$ and mAbp1$^{+/+}$ PMNs was studied with *E coli* opsonized with serum from recombination activating gene 1–deficient mice that are characterized by a T- and B-cell maturation defect and a subsequent lack of IgG.[23] With the use of this approach, phagocytosis was found to be significantly impaired in mAbp1$^{-/-}$ PMNs compared with control cells (data not shown), indicating that the observed effect was specific for β_2 integrin–mediated phagocytosis.

Role of Syk for proper localization of mAbp1 and phagocytosis

The nonreceptor tyrosine kinase Syk is essential for FcγR-mediated phagocytosis in macrophages and PMNs, but it seems to be dispensable for β_2 integrin–mediated phagocytosis in macrophages.[32] Unexpectedly, Shi et al[18] have shown that Syk was required for β_2 integrin–mediated phagocytosis in dHL-60 cells.[18] To test whether the genetic absence of mAbp1 affects Syk expression or stability, we measured the expression of Syk semiquantitatively by Western blot technique, but we found no difference between murine mAbp1$^{-/-}$ and mAbp1$^{+/+}$ PMNs (supplemental Figure 5). Because Syk is required for the formation and/or stabilization of signaling complexes,[19,25,33] we analyzed the subcellular localization of mAbp1 in murine Syk$^{-/-}$ and Syk$^{+/+}$ PMNs. The genetic absence of Syk abrogated the enrichment of mAbp1 at the site of particle binding (Figure 3A). Similar results were obtained on pharmacologic inhibition of Syk with the Syk inhibitor piceatannol (Figure 3B). However, piceatannol did not affect the colocalization between *E coli* and CD18, suggesting that particle binding was still intact and independent of Syk activity (Figure 3C).

Similar to mAbp1, Syk was enriched in murine PMNs and dHL-60 cells at the site of particle binding, and the genetic absence of Syk or its pharmacologic inhibition with piceatannol did not interfere with particle binding (Figure 4A-B). However, the localization of Syk at the site of particle binding was abrogated on inhibition of Syk (Figure 4B). Those Syk molecules that were localized at the site of particle binding were phosphorylated as detected by a specific anti–phosho-Syk antibody (Figure 4C). On

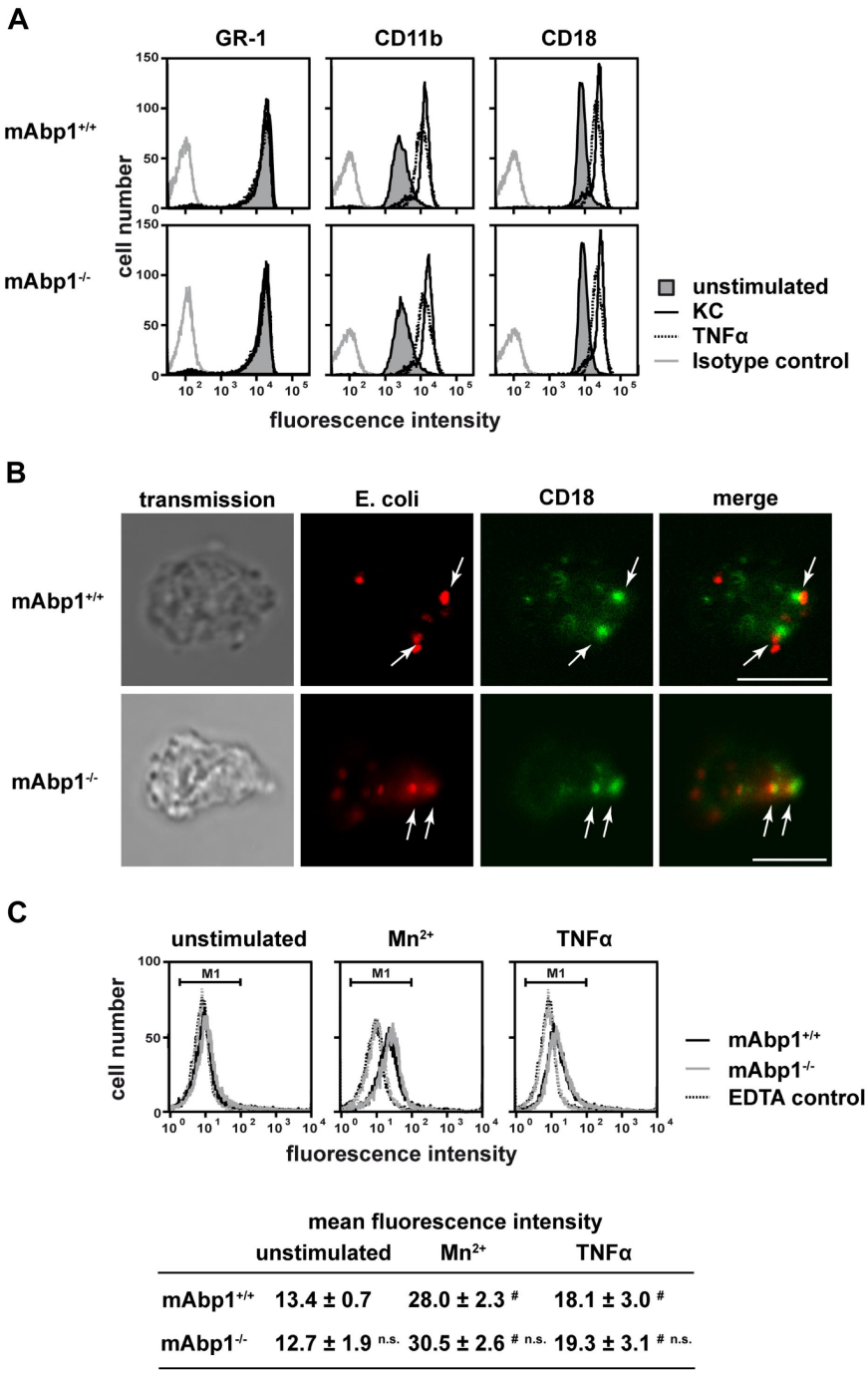

Figure 2. No effect of mAbp1 on β_2 integrin expression, up-regulation, and localization during phagocytosis or fibrinogen binding. (A) Flow cytometric analysis of cell-surface expression of GR-1, CD11b, and CD18 in mAbp1$^{+/+}$ or mAbp1$^{-/-}$ PMNs stimulated with KC (100 ng/mL), TNFα (100 ng/mL), or left unstimulated. (B) Confocal microscopy images of murine PMNs phagocytosing serum-opsonized Alexa 594–conjugated *E coli* (red). Translocation of CD18 (green) to the site of particle binding (arrows) was not affected in Abp1$^{-/-}$ PMNs. Bar = 10 μm. Data are representative for 3 independent experiments. (C) Binding of Alexa 488–conjugated fibrinogen to murine mAbp1$^{+/+}$ and mAbp1$^{-/-}$ PMNs as measured by flow cytometry. Cells were incubated for 20 minutes with EDTA as negative control, Mn^{2+} (3 mM), TNFα (100 ng/mL), or left unstimulated. Addition of 1 mM Mn^{2+} gave similar results (data not shown). Mean fluorescence intensity within marker 1 (M1) ± SD; n = 4; #$P < .05$ versus unstimulated control; n.s. indicates not significant versus wild-type control.

mean fluorescence intensity	unstimulated	Mn^{2+}	TNFα
mAbp1$^{+/+}$	13.4 ± 0.7	28.0 ± 2.3 #	18.1 ± 3.0 #
mAbp1$^{-/-}$	12.7 ± 1.9 n.s.	30.5 ± 2.6 # n.s.	19.3 ± 3.1 # n.s.

inhibition of Syk with piceatannol, phosphorylated Syk was not detectable in dHL-60 cells, confirming the efficient inhibition of the kinase. In accordance with a previous study,[18] complement-mediated phagocytosis was significantly impaired in dHL-60 cells compared with control cells (100%) on pharmacologic or genetic down-regulation of Syk with piceatannol or the RNAi technique (Figure 4D-E). An open question so far has been the effect of Syk for complement-mediated phagocytosis in native PMNs. To address this question, we measured phagocytosis in Syk$^{-/-}$ PMNs and found that it was substantially impaired compared with Syk$^{+/+}$ PMNs within 10 minutes and 20 minutes after the onset of the experiment (Figure 4F). These results indicated that β_2 integrin–mediated outside-in signaling during complement-mediated phagocytosis required Syk in PMNs.

Effect of mAbp1 for firm adhesion under flow conditions in vitro and in inflamed cremaster muscle venules in mice

Next, we studied adhesion of murine mAbp1$^{-/-}$ and mAbp1$^{+/+}$ PMNs on immobilized fibrinogen or ICAM-1 in a static adhesion assay. On induction of adhesion by TNFα (100 ng/mL) or Mn^{2+} (1 mM), which is known to stabilize integrins in their active conformation,[34] mAbp1$^{+/+}$ PMNs showed a significant increase of adhesion on immobilized fibrinogen (Figure 5A) and ICAM-1 (Figure 5B), which was also true for mAbp1$^{-/-}$ PMNs, showing that mAbp1 was not required for β_2 integrin–mediated adhesion under static conditions in vitro. To investigate a potential contribution of mAbp1 in leukocyte recruitment in vivo, we studied leukocyte rolling and adhesion in 33 TNFα-stimulated cremaster

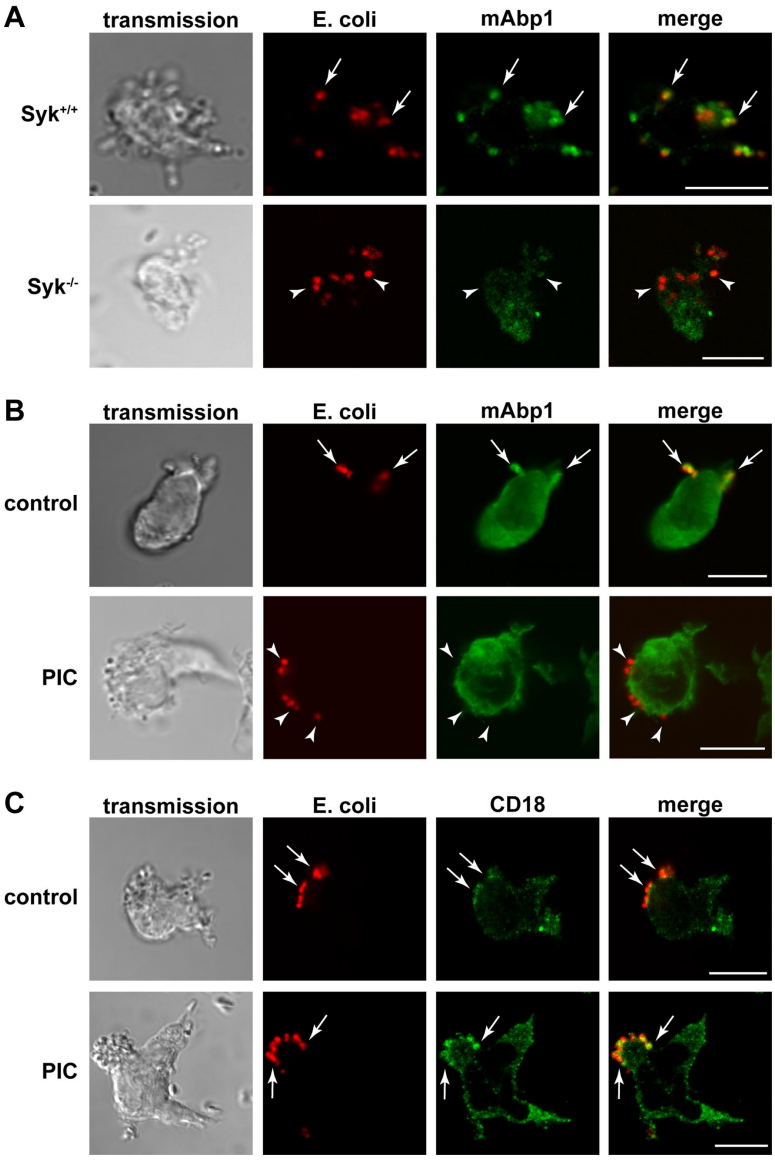

Figure 3. Syk was required for the translocation of mAbp1 to the site of particle binding. Confocal microscopy images of (A) murine $Syk^{+/+}$ and $Syk^{-/-}$ PMNs and (B-C) piceatannol-treated (PIC) and untreated (control) dHL-60 cells phagocytosing serum-opsonized Alexa 594–conjugated *E coli* (red). (A) Translocation of mAbp1 (green) to the site of particle binding was severely compromised in $Syk^{-/-}$ PMNs (arrowheads) compared with $Syk^{+/+}$ PMNs in which mAbp1 was distinctly enriched at the site of particle binding (arrows). (B) On inhibition of Syk with 30μM piceatannol (PIC), the translocation of mAbp1 to the site of particle binding was impaired (arrowheads) compared with DMSO-treated dHL-60 control cells (arrows). (C) Translocation of CD18 (green) to the site of particle binding was not affected by the inhibition of Syk (↑, ↓) in dHL-60 cells. Images are representative for 3 independent experiments. Bar = 10 μm.

muscle venules of 5 $mAbp1^{-/-}$ mice and compared it to 27 TNFα-stimulated cremaster muscle venules of 5 $mAbp1^{+/+}$ mice. Microvascular parameters during the intravital microscopy experiments were comparable between the 2 groups (Table 1). Two hours after intrascrotal injection of TNFα, leukocyte rolling is dependent on P-selectin and E-selectin.[28] We found no significant difference in rolling flux fractions between $mAbp1^{-/-}$ mice (9% ± 1%) and $mAbp1^{+/+}$ mice (11% ± 1%; Figure 5C), suggesting normal rolling behavior in $mAbp1^{-/-}$ mice. Next, we analyzed leukocyte adhesion in TNFα-stimulated cremaster muscle venules. In contrast to the results from the static in vitro assay, leukocyte adhesion was significantly reduced by 79% in $mAbp1^{-/-}$ mice (175 ± 16 cells/mm^2) compared with $mAbp1^{+/+}$ mice (815 ± 71 cells/mm^2; Figure 5D), pointing toward a severe impairment in firm leukocyte adhesion under in vivo conditions. To further characterize the observed defect, we assessed leukocyte rolling velocities in TNFα-treated cremaster muscle venules of $mAbp1^{-/-}$ mice and $mAbp1^{+/+}$ mice. As shown in Figure 5E, we found no difference in the distribution of rolling velocities between $mAbp1^{-/-}$ mice (average rolling velocity, 5.2 ± 0.6 μm/s; n = 57) and $mAbp1^{+/+}$ mice (average rolling velocity, 5.5 ± 0.6 μm/s; n = 64), suggesting that β_2 integrin–dependent slow leukocyte rolling on the inflamed endothelium that requires the intermediate affinity of the β_2 integrins did not depend on mAbp1.[20] Next, we assessed the number of intravascular and perivascular leukocytes from whole-mount histologic preparations of TNFα-treated cremaster muscles from $mAbp1^{-/-}$ mice (73 venules of 8 cremaster muscles) and $mAbp1^{+/+}$ mice (68 venules of 8 cremaster muscles). Similar to the intravital microscopic experiments, we found a significant decrease in the number of intravascular leukocytes in cremaster muscle venules of $mAbp1^{-/-}$ mice (630 ± 40 cells/mm^2) compared with $mAbp1^{+/+}$ mice (1560 ± 120 cells/mm^2; Figure 5F). In addition, the number of perivascular leukocytes was also significantly decreased in $mAbp1^{-/-}$ mice (120 ± 10 cells/mm^2) compared with $mAbp1^{+/+}$ mice (300 ± 30 cells/mm^2), confirming that leukocyte adhesion to the vessel wall, and accumulation in the tissue was dramatically impaired in $mAbp1^{-/-}$ mice in vivo.

mAbp1 was indispensable for leukocyte adhesion under dynamic conditions in vitro

To test whether the observed adhesion defect was caused by the absence of mAbp1 in leukocytes, we analyzed adhesion under flow conditions in a reductionist system, namely a previously described ex vivo microflow

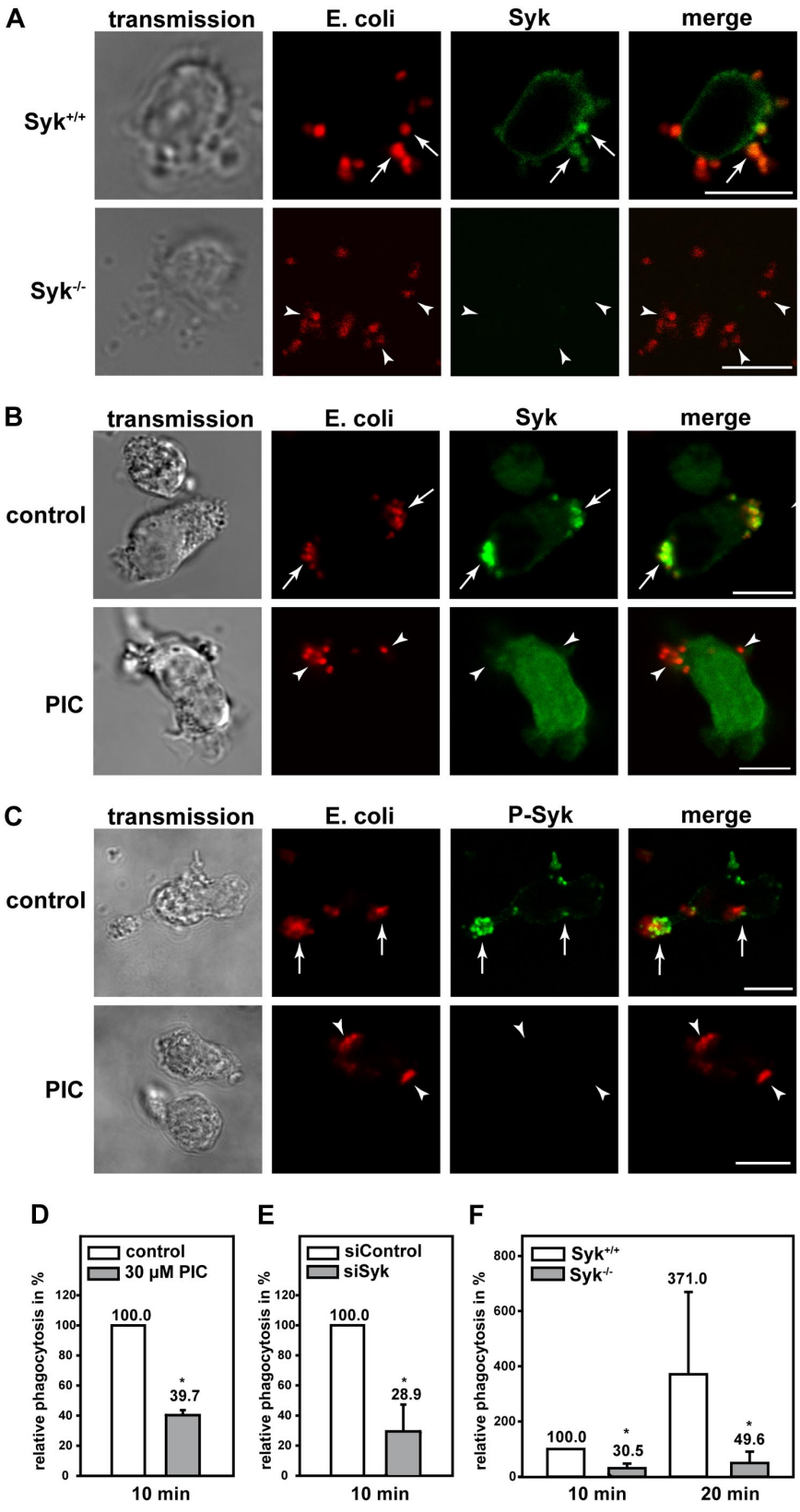

Figure 4. Syk was required for efficient β_2 integrin–mediated phagocytosis of serum-opsonized *E coli*. Confocal microscopy images of (A) murine Syk$^{+/+}$ and Syk$^{-/-}$ PMNs and (B-C) piceatannol-treated (PIC) and untreated (control) dHL-60 cells phagocytosing serum-opsonized Alexa 594–conjugated *E coli* (red). Syk was enriched at the site of particle binding (arrows) in murine Syk$^{+/+}$ PMNs (A) and in dHL-60 control cells (B). (B) In contrast, Syk was not translocated in cells after the inhibition of Syk by 30μM piceatannol (PIC, arrowheads). (C) Syk was activated at the site of particle binding, assessed by a specific anti–phospho-Syk antibody (P-Syk). (A,C) As expected no Syk or P-Syk staining was detected in Syk$^{-/-}$ PMNs or piceatannol-treated dHL-60 cells, respectively (arrowheads). Results shown are representative for 3 independent experiments. Bar = 10 μm. Phagocytosis of serum-opsonized Alexa 594–conjugated *E coli* by dHL-60 cells (D) after pharmacologic inhibition of Syk with 30μM piceatannol (PIC) or (E) genetic down-regulation with the RNAi technique (siSyk) compared with control cells (100%; control or siControl, respectively). (F) Phagocytosis of murine Syk$^{+/+}$ or Syk$^{-/-}$ PMNs. (D-F) Mean relative phagocytosis ± SD; n = 4; $^*P < .05$.

chamber.[35] The microflow chambers were coated with P-selectin, ICAM-1, and KC, which binds to CXCR1 and CXCR2. Blood flow velocities in the flow chambers were similar between mAbp1$^{-/-}$ mice (1.5 ± 0.1 mm/s; 18 chambers in 5 mice) and mAbp1$^{+/+}$ mice (1.6 ± 0.04 mm/s; 28 chambers in 9 mice). We found that the number of adherent cells per field of view (FOV) assessed after 8 minutes of perfusion was significantly reduced in mAbp1$^{-/-}$ mice (6 ± 2 cells/FOV) compared with mAbp1$^{+/+}$ mice (11 ± 3 cells/FOV; $P < .05$; Figure 6A), showing that the adhesion defect was still present in the reductionist model. The observed persistence of the adhesion defect

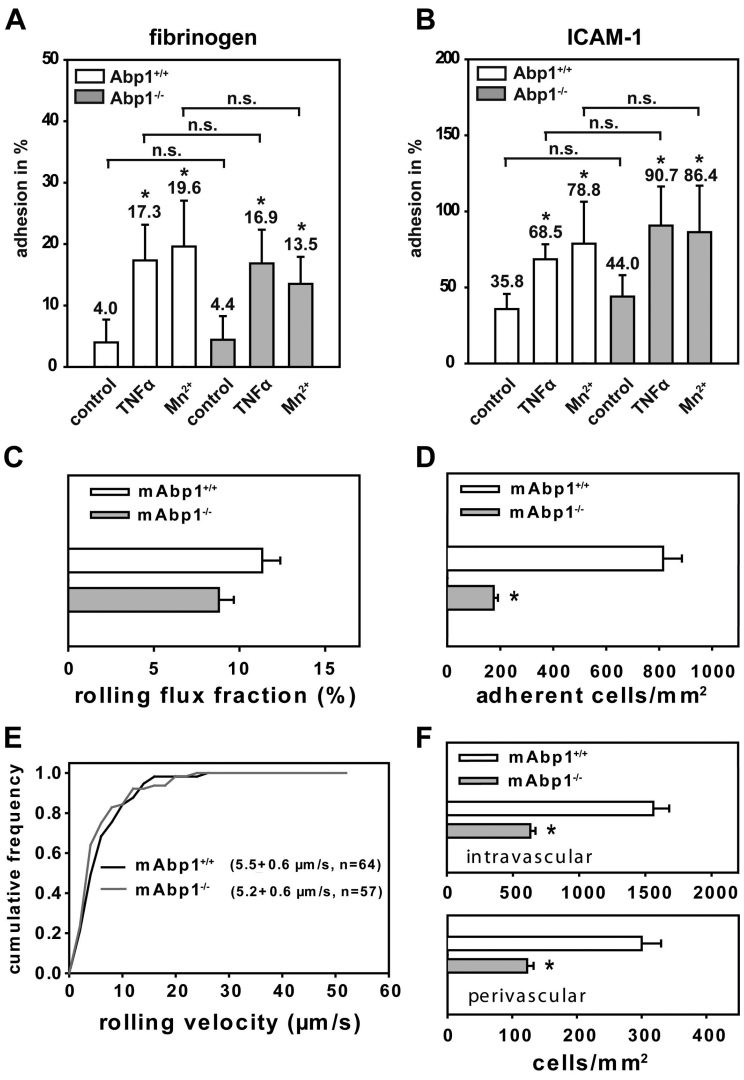

Figure 5. Leukocyte adhesion was impaired in the absence of mAbp1 under flow conditions in vivo. Adhesion of mAbp1$^{+/+}$ and mAbp1$^{-/-}$ PMNs under static conditions on immobilized (A) fibrinogen or (B) ICAM-1 30 minutes after treatment with TNFα (100 ng/mL) or Mn^{2+} (1 mM). Data represent adhesion in percentage of cells adherent to poly-L-lysine (100%). Means ± SDs; mAbp1$^{+/+}$, n = 5; mAbp1$^{-/-}$, n = 4; *$P < .05$ versus unstimulated control; n.s. indicates not significant. Intravital microscopic analysis of PMNs (C) rolling (leukocyte rolling flux fraction; mean percentage ± SEM) and (D) adhesion (means of adherent cells/mm^2 ± SEMs) in TNFα-stimulated cremaster muscle venules of mAbp1$^{+/+}$ (□) and mAbp1$^{-/-}$ mice (▨). (E) Cumulative frequency distribution of leukocyte rolling velocities in mAbp1$^{+/+}$ mice (black line) and mAbp1$^{-/-}$ (gray line). (F) Quantitative analysis of intravascular and perivascular leukocytes in whole-mount TNFα-treated cremaster muscle preparations from mAbp1$^{+/+}$ mice (□) and mAbp1$^{-/-}$ (▨). Means of cells/mm^2 ± SEMs; n = 5; *$P < .05$.

even in the absence of endothelial cells strongly indicated that this defect was due to the indispensable role of leukocyte mAbp1 for adhesion under flow conditions. As expected, immobilizing P-selectin alone, KC in combination with ICAM-1, or using flow chambers without any immobilized proteins did not lead to sufficient adhesion in the chamber.

Next, we tested the hypothesis that the impairment of adhesion in the absence of mAbp1$^{-/-}$ was caused by an impaired resistance of adherent PMNs against shear stress. Therefore, we performed detachment assays with isolated PMNs from mAbp1$^{-/-}$ mice and mAbp1$^{+/+}$ mice. Microflow chambers were coated with P-selectin, ICAM-1, and KC. After filling the chamber with perfusion buffer containing 10^6 PMNs/mL, cells were kept in the chamber without flow to settle down and adhere. After 4 minutes, flow was started at 0.1 dyne/cm^2 to rinse unattached cells away, and the numbers of adherent cells per FOV were defined as 100%. Thereafter, flow was increased every 30 seconds to a maximum shear stress level of 16 dynes/cm^2 as described in "Autoperfused microflow chamber" in the supplemental Methods. The decrease in PMN adhesion observed at intermediate shear stress levels was much more pronounced in the absence of mAbp1 (Figure 6B). These results suggest that mAbp1 was crucial for stabilizing PMN adhesion under shear stress to protect PMNs from getting flushed away by the exerted shear forces.

In analogy to the observed shear stress–dependent defect of PMN adhesion in mAbp1$^{-/-}$ mice in the dynamic flow chamber assay, we compared leukocyte adhesion in TNFα-stimulated cremaster muscle venules from mAbp1$^{-/-}$ mice and mAbp1$^{+/+}$ mice in relation to shear rate. Two shear rate classes (intermediate shear

Table 1. Microvascular parameters of TNFα -treated cremaster muscle venules of mAbp1$^{+/+}$ and mAbp1$^{-/-}$ mice

	Mice, n	Venules, n	Diameter, μm	Centerline velocity, μm/s	Shear rate, s^{-1}	WBC, μL^{-1}
mAbp1$^{+/+}$	5	27	35 ± 1	1400 ± 80	1000 ± 70	2600 ± 400
mAbp1$^{-/-}$	5	33	32 ± 1	1600 ± 140	1200 ± 100	2400 ± 200
			ns	ns	ns	ns

Mean ± SEM.
ns indicates not significant; and WBC, white blood cell counts.

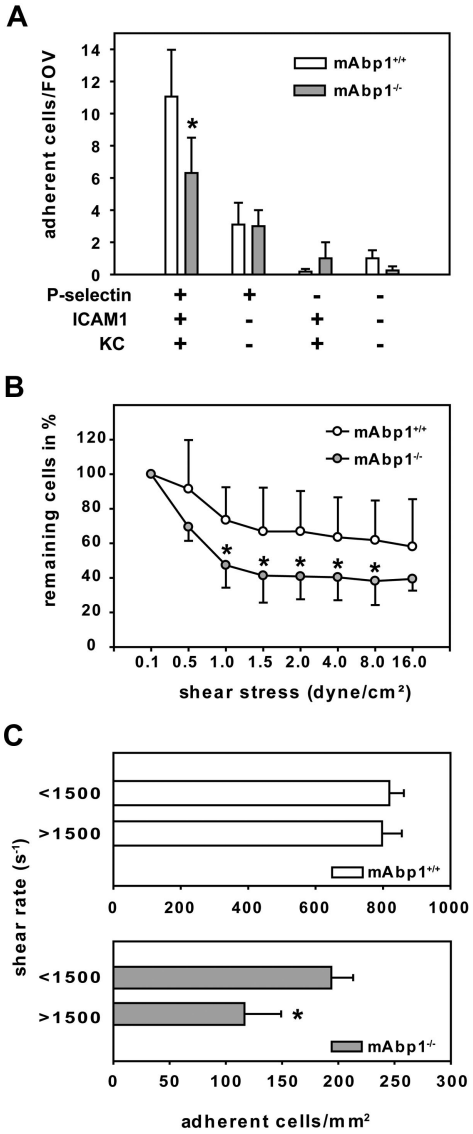

Figure 6. mAbp1 expression in leukocytes was required for leukocyte firm adhesion. (A) Ex vivo microflow chambers coated with recombinant murine (rm) P-selectin, rmICAM-1, and rmKC were perfused with whole blood from mAbp1$^{+/+}$ (n = 9) or mAbp1$^{-/-}$ (n = 5) mice. Leukocyte adhesion was assessed after 8 minutes of perfusion. Mean number of adherent cells/FOV ± SEM (B) In vitro detachment assay of mAbp1$^{+/+}$ (○) and mAbp1$^{-/-}$ (●) PMNs perfused through a rmP-selectin–, rmICAM-1–, and rmKC-coated flow chamber at gradually increasing shear stress levels. Initial cell number at 0.1 dyn/cm^2 was set to 100%. Relative adherent cells/FOV in mean ± SD; n = 7. (C) Leukocyte adhesion in TNFα-treated cremaster muscle venules of mAbp1$^{+/+}$ (□) and mAbp1$^{-/-}$ (■) mice with medium shear rate (< 1500 s^{-1}) and high shear rate (> 1500 s^{-1}). Means of adherent leukocytes/mm^2 ± SEMs; n = 5; *$P < .05$.

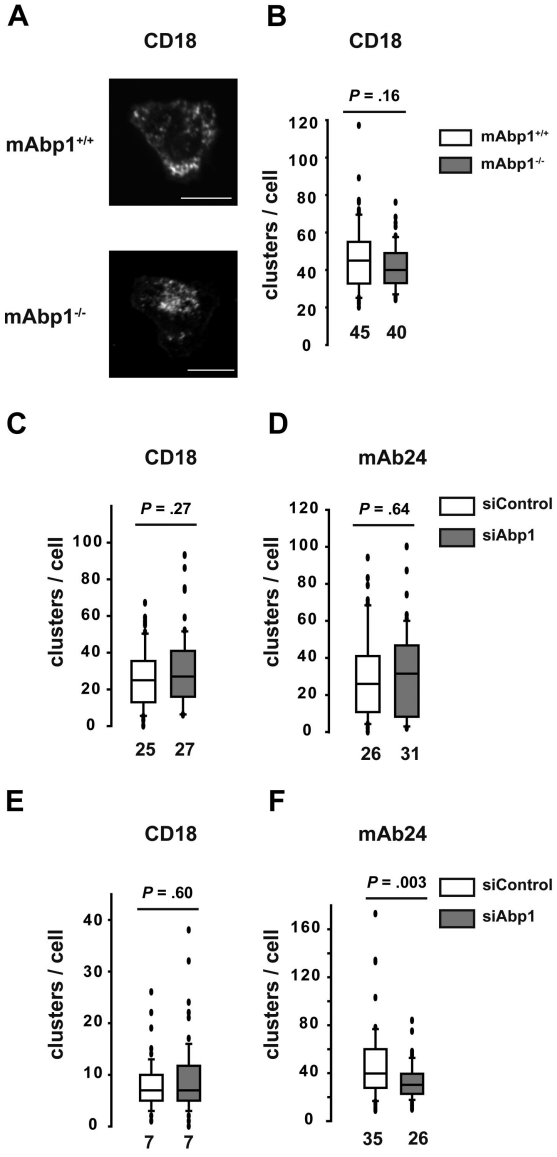

Figure 7. Effect of mAbp1 on the high-affinity conformation of β_2 integrins under flow conditions. (A) Confocal microscopy images of mAbp1$^{+/+}$ and mAbp1$^{-/-}$ PMNs adherent on immobilized ICAM-1 on stimulation with 1μM fMLP stained for CD18. Box whisker blots of numbers of clusters of CD18 clusters in all 3 conformations (CD18) (B-C,E) or CD18 clusters in the high-affinity conformation (mAb24) (D,F), under static (B-D) or flow (E-F) conditions (0.5 dyne/cm^2). Median numbers are indicated; n = 3.

rate, < 1500 s^{-1}; high shear rate, > 1500 s^{-1}) were formed for each group. As shown in Figure 6C, we found no difference in the number of adherent control leukocytes between the intermediate and high shear rates in mAbp1$^{+/+}$ mice. In contrast, in mAbp1$^{-/-}$ mice, leukocyte adhesion was significantly higher in the intermediate class than in the high shear rate class, confirming a shear-dependent adhesion defect in mAbp1$^{-/-}$ mice.

Effect of mAbp1 on the reinforcement of the high-affinity conformation of the β_2 integrins under flow conditions

An essential role for adhesion strengthening in PMNs under flow conditions has been shown for WASP by controlling integrin clustering.[36] However, no significant difference in the subcellular localization of WASP was detectable in adherent mAbp1$^{-/-}$ PMNs or siAbp1 dHL-60 cells compared with control cells. This was true for static and flow conditions (supplemental Figure 6). Next, we studied integrin clustering in murine PMNs and dHL-60 cells during static conditions with the use of confocal microscopy, followed by an offline analysis of the images in a blinded manner. Murine mAbp1$^{+/+}$ and mAbp1$^{-/-}$ PMNs adherent on immobilized ICAM-1 showed CD18 clustering after stimulation with fMLP (1μM) under static conditions as determined by CD18 antibody staining (Figure 7A). However, there was no difference in the number of clusters per cell between mAbp1$^{+/+}$ and mAbp1$^{-/-}$ PMNs (Figure 7B). Similarly, we found no difference in CD18 clustering between mAbp1$^{+/+}$ and mAbp1$^{-/-}$ PMNs after stimulation by 100 ng/mL KC on exposure to immobilized fibrinogen or ICAM-1 (data

not shown). In accordance with the results obtained in the murine system, CD18 clustering in dHL-60 cells that adhered on immobilized ICAM-1 was not affected on the down-regulation of mAbp1 with the use of the RNAi technique (Figure 7C). Thus, unlike WASP$^{-/-}$ PMNs that showed impaired clustering of LFA-1 and Mac-1 under static conditions,[36] the absence or down-regulation of mAbp1 did not interfere with integrin clustering under static conditions. Because β_2 integrins exist in 3 different conformations (an inactive or bended form and 2 active, extended forms, the intermediate and the high-affinity conformation[34]), we measured the effect of mAbp1 on the high-affinity conformation, which is critical for adhesion under flow conditions.[37] With the use of the monoclonal antibody mAb24 that specifically detects the high-affinity conformation of the β_2 integrins,[38] we found no difference in the number of mAb24-positive clusters per cell on immobilized ICAM-1 under static conditions on down-regulation of mAbp1 with the RNAi technique (Figure 7D). Next, we analyzed integrin clustering after the application of a shear stress of 0.5 dyn/cm^2 for 10 minutes in a flow chamber. Similar to static conditions, the number of CD18 clusters per cell was not affected on down-regulation of mAbp1 (Figure 7E). However, the number of mAb24-positive clusters was significantly decreased in siAbp1 dHL-60 cells compared with control cells, indicating an effect of mAbp1 for reinforcement of the high-affinity conformation of β_2 integrins under flow conditions, which may explain the adhesion defect in the flow chamber and in the situation in vivo (Figure 7F). In summary, mAbp1 seems to be of fundamental importance for β_2 integrin–mediated PMN engulfment of bacteria and the resistance against shear forces during firm PMN adhesion to the vessel wall that represents a predominant requirement for PMN extravasation. Thus, the present study provides evidence for a widely unanticipated but fundamental role of mAbp1 in neutrophil biology.

Discussion

In this study, we have identified mAbp1 function as a novel molecular requirement for firm PMN adhesion under flow conditions and for phagocytosis of complement-opsonized *E coli* particles. The unanticipated finding that phagocytosis was impaired in mAbp1$^{-/-}$ PMNs was not due to a down-regulation of the complement-receptor Mac-1 or compromised PMN differentiation as defined by the expression the PMN differentiation marker GR-1. These findings suggest that mAbp1 exerts its function directly as a component of the molecular mechanism underlying phagocytosis. Phagocytosis is usually mediated by multiple receptors that induce different cooperating signaling pathways simultaneously.[30] In our experimental settings, phagocytosis was strictly dependent on β_2 integrins, because engulfment of serum-opsonized *E coli* particles was almost absent in CD18-deficient PMNs or in the presence of heat-inactivated serum. The relevance of our findings for host defense against pathogens was shown with the use of *S typhimurium* as a model for bacterial infection. *S typhimurium* causes systemic infections in mice, and PMNs are critically involved in the early host defense against *S typhimurium* infection.[39] With the use of this model, we provided evidence that mAbp1 was critical for innate control of bacterial infection in vivo. Moreover, we found that complement-mediated phagocytosis depended on Syk in native murine PMNs. This finding is in accordance with a previous study showing reduced phagocytosis of iC3b-opsonized zymosan particles in dHL-60 cells on a down-regulation of Syk expression by the RNAi technique.[18] In addition, we have shown that Syk was required for the translocation of mAbp1 to the site of particle binding during complement-mediated phagocytosis in dHL-60 cells and native murine PMNs. During this process, Syk may be involved in the establishment and stabilization of a signaling complex at the site of particle binding as shown earlier for the stabilization of the leading edge and efficient cell migration in PMNs.[19,25]

One of the most unexpected and important findings of this study was that mAbp1$^{-/-}$ PMNs showed a severe defect in firm arrest in the inflamed cremaster muscle and in a flow chamber assay in vitro. Similarly, adhesion of Syk$^{-/-}$ PMNs in fMLP-stimulated cremaster muscle venules was impaired.[16] In contrast to mAbp1$^{-/-}$ PMNs, in which adhesion and spreading were unaffected under static conditions compared with wild-type control cells, adhesion and spreading of Syk$^{-/-}$ PMNs under static conditions were severely compromised, indicating that Syk is required for β_2 integrin–mediated outside-in signaling under static conditions.[16,17] Because we observed no differences in rolling flux fractions or rolling velocity of mAbp1$^{-/-}$ compared with mAbp1$^{+/+}$ PMNs, the adhesion defect of mAbp1$^{-/-}$ PMNs under flow conditions was obviously not due to defective selectin or selectin ligand function required for leukocyte rolling. The microflow chamber experiments showed that the observed effect was caused by the absence of mAbp1 in PMNs. Further analyses showed that the absence of mAbp1 interfered with the ability of the adherent leukocytes to resist shear forces. The biologic consequences of the observed defect became evident by measuring intravascular and perivascular PMN accumulation in the inflamed cremaster model in which PMN recruitment was found to be dramatically compromised.

During firm arrest under flow conditions, the complex regulation of β_2 integrin affinity involves integrin activation induced by chemokines and a reinforcement of integrin affinity by outside-in signaling.[37] An essential role for adhesion strengthening in PMNs has been shown for WASP.[36] Interestingly, the described defects of WASP$^{-/-}$ PMNs closely resembled the functional abnormalities of the mAbp1$^{-/-}$ PMNs because WASP$^{-/-}$ PMNs failed to perform firm arrest under shear stress, whereas cell adhesion was not affected under static conditions.[36] Although, WASP did not colocalize with β_2 integrins in murine PMNs, Zhang et al[36] have shown impaired integrin clustering in adherent WASP$^{-/-}$ PMNs in the absence of shear stress. In a comparable setting, no difference in the number of β_2 integrin clusters per cell was detectable in the absence of mAbp1, suggesting that this molecule was not required for β_2 integrin clustering under static conditions. In addition, the up-regulation of β_2 integrin expression at the cell surface after stimulation with KC or TNFα was not altered in mAbp1$^{-/-}$ PMNs, indicating that exocytosis of specific granules and secretory vesicles was independent of mAbp1. However, the number of β_2 integrin clusters in the high-affinity conformation was reduced under shear stress. This finding bears physiologic relevance because the β_2 integrins in the high-affinity conformation are the main mediators of cell adhesion.[34] The different integrin conformations are thought to be in equilibrium that is shifted toward the high-affinity conformation by external forces, for example, in T cells and PMNs in which shear stress facilitated optimal integrin activation.[34,40] To withstand external forces, the integrins have to be properly anchored to the cytoskeleton.[37] In its extended conformation, LFA-1 is mobile in the cell membrane of Jurkat cells unless

the receptor binds ICAM-1 and becomes immobilized by cytoskeletal linkage.[41] T cells control the activity of LFA-1 by altering the equilibrium between mobile and cytoskeletally confined receptor pools, a process that involves cytoskeletal regulators.[41] Thus, mAbp1 may be involved in shifting this equilibrium toward the high-affinity conformation, a prerequisite to withstand external forces during firm adhesion under flow conditions. In summary, we found that mAbp1 has a fundamental effect on PMN functions that are mediated by β_2 integrins and depend on the generation of tension, namely the ability of the cell to adhere under flow conditions as well as the engulfment of opsonized bacteria. Thus, mAbp1 represents a novel linker molecule that connects the β_2 integrin function to the actin cytoskeleton, enabling the cell to withstand shear forces during adhesion under flow or to generate tensile strength during particle engulfment.

Acknowledgments

We thank Dr Nancy Hogg (Leukocyte Adhesion Laboratory, Cancer Research UK London Research Institute, London, United Kingdom) for providing the mAb24 antibody.

This work was supported by grants of the Deutsche Forschungsgemeinschaft (Wa 1048/2-3 to B.W., SP621/3-1 to M. Sperandio, and SFB 523 to J.W.).

Authorship

Contribution: B.W. designed the research, analyzed data, and wrote the manuscript; J.S. designed and carried out the research, analyzed data, and wrote the manuscript; R.G., I.M., and K.N. performed research and analyzed data; D.F. performed the in vivo experiments with the inflamed cremaster muscle model and the autoperfused microflow chamber and analyzed data; M. Sperandio designed the research, analyzed data, and wrote the intravital microscopy part of the manuscript; K.P. performed the in vitro phagocytosis of *S typhimurium* and the clearance of bacterial infection in vivo and analyzed data; M. Sixt performed spinning disc microscopy and analyzed data; T.Q. performed confocal scanning microcopy and processed data for 3D animation; A.M. and J.W. contributed analytical tools and edited the manuscript; and W.K. and J.H. designed the research and edited the manuscript.

Conflict-of-interest disclosure: The authors declare no competing financial interests.

Correspondence: Barbara Walzog, Department of Cardiovascular Physiology and Pathophysiology, Walter Brendel Centre for Experimental Medicine, Ludwig-Maximilians-University Munich, Schillerstr 44, D-80336 Munich, Germany; e-mail: walzog@lrz.uni-muenchen.de.

References

1. Larbolette O, Wollscheid B, Schweikert J, Nielsen PJ, Wienands J. SH3P7 is a cytoskeleton adapter protein and is coupled to signal transduction from lymphocyte antigen receptors. *Mol Cell Biol.* 1999;19(2):1539-1546.
2. Kessels MM, Engqvist-Goldstein AE, Drubin DG. Association of mouse actin-binding protein 1 (mAbp1/SH3P7), an Src kinase target, with dynamic regions of the cortical actin cytoskeleton in response to Rac1 activation. *Mol Biol Cell.* 2000; 11(1):393-412.
3. Han J, Kori R, Shui JW, Chen YR, Yao Z, Tan TH. The SH3 domain-containing adaptor HIP-55 mediates c-Jun N-terminal kinase activation in T cell receptor signaling. *J Biol Chem.* 2003;278(52): 52195-52202.
4. Larive RM, Urbach S, Poncet J, et al. Phosphoproteomic analysis of Syk kinase signaling in human cancer cells reveals its role in cell-cell adhesion. *Oncogene.* 2009;28(24):2337-2347.
5. Goode BL, Rodal AA, Barnes G, Drubin DG. Activation of the Arp2/3 complex by the actin filament binding protein Abp1p. *J Cell Biol.* 2001;153(3): 627-634.
6. Pinyol R, Haeckel A, Ritter A, Qualmann B, Kessels MM. Regulation of N-WASP and the Arp2/3 complex by Abp1 controls neuronal morphology. *PLoS One.* 2007;2(5):e400.
7. Kessels MM, Engqvist-Goldstein AE, Drubin DG, Qualmann B. Mammalian Abp1, a signal-responsive F-actin-binding protein, links the actin cytoskeleton to endocytosis via the GTPase dynamin. *J Cell Biol.* 2001;153(2):351-366.
8. Connert S, Wienand S, Thiel C, et al. SH3P7/mAbp1 deficiency leads to tissue and behavioral abnormalities and impaired vesicle transport. *EMBO J.* 2006;25(8):1611-1622.
9. Han J, Shui JW, Zhang X, Zheng B, Han S, Tan TH. HIP-55 is important for T-cell proliferation, cytokine production, and immune responses. *Mol Cell Biol.* 2005;25(16):6869-6878.
10. Onabajo OO, Seeley MK, Kale A, et al. Actin-binding protein 1 regulates B cell receptor-mediated antigen processing and presentation in response to B cell receptor activation. *J Immunol.* 2008;180(10):6685-6695.
11. Ley K, Laudanna C, Cybulsky MI, Nourshargh S. Getting to the site of inflammation: the leukocyte adhesion cascade updated. *Nat Rev Immunol.* 2007;7(9):678-689.
12. Yan SR, Huang M, Berton G. Signaling by adhesion in human neutrophils: activation of the p72syk tyrosine kinase and formation of protein complexes containing p72syk and Src family kinases in neutrophils spreading over fibrinogen. *J Immunol.* 1997;158(4):1902-1910.
13. Willeke T, Behrens S, Scharffetter-Kochanek K, Gaehtgens P, Walzog B. Beta2 integrin (CD11/CD18)-mediated signaling involves tyrosine phosphorylation of c-Cbl in human neutrophils. *J Leukoc Biol.* 2000;68(2):284-292.
14. Willeke T, Schymeinsky J, Prange P, Zahler S, Walzog B. A role for Syk-kinase in the control of the binding cycle of the beta2 integrins (CD11/CD18) in human polymorphonuclear neutrophils. *J Leukoc Biol.* 2003;74(2):260-269.
15. Mocsai A, Abram CL, Jakus Z, Hu Y, Lanier LL, Lowell CA. Integrin signaling in neutrophils and macrophages uses adaptors containing immunoreceptor tyrosine-based activation motifs. *Nat Immunol.* 2006;7(12):1326-1333.
16. Frommhold D, Mannigel I, Schymeinsky J, et al. Spleen tyrosine kinase Syk is critical for sustained leukocyte adhesion during inflammation in vivo. *BMC Immunol.* 2007;8:31.
17. Mocsai A, Zhou M, Meng F, Tybulewicz VL, Lowell CA. Syk is required for integrin signaling in neutrophils. *Immunity.* 2002;16(4):547-558.
18. Shi Y, Tohyama Y, Kadono T, et al. Protein-tyrosine kinase Syk is required for pathogen engulfment in complement-mediated phagocytosis. *Blood.* 2006;107(11):4554-4562.
19. Schymeinsky J, Then C, Sindrilaru A, et al. Syk-mediated translocation of PI3Kd to the leading edge controls lamellipodium formation and migration of leukocytes. *PLoS One.* 2007;2(11):e1132.
20. Zarbock A, Lowell CA, Ley K. Spleen tyrosine kinase Syk is necessary for E-selectin-induced alpha (L)beta(2) integrin-mediated rolling on intercellular adhesion molecule-1. *Immunity.* 2007; 26(6):773-783.
21. Le Bras S, Foucault I, Foussat A, Brignone C, Acuto O, Deckert M. Recruitment of the actin-binding protein HIP-55 to the immunological synapse regulates T cell receptor signaling and endocytosis. *J Biol Chem.* 2004;279(15):15550-15560.
22. Turner M, Mee PJ, Costello PS, et al. Perinatal lethality and blocked B-cell development in mice lacking the tyrosine kinase Syk. *Nature.* 1995; 378(6554):298-302.
23. Mombaerts P, Iacomini J, Johnson RS, Herrup K, Tonegawa S, Papaioannou VE. RAG-1-deficient mice have no mature B and T lymphocytes. *Cell.* 1992;68(5):869-877.
24. Scharffetter-Kochanek K, Lu H, Norman K, et al. Spontaneous skin ulceration and defective T cell function in CD18 null mice. *J Exp Med.* 1998; 188(1):119-131.
25. Schymeinsky J, Sindrilaru A, Frommhold D, et al. The Vav binding site of the non-receptor tyrosine kinase Syk at Tyr 348 is critical for beta2 integrin (CD11/CD18)-mediated neutrophil migration. *Blood.* 2006;108(12):3919-3927.
26. Kaniga K, Bossio JC, Galan JE. The *Salmonella typhimurium* invasion genes invF and invG encode homologues of the AraC and PulD family of proteins. *Mol Microbiol.* 1994;13(4):555-568.
27. Hoiseth SK, Stocker BA. Aromatic-dependent *Salmonella typhimurium* are non-virulent and effective as live vaccines. *Nature.* 1981;291(5812): 238-239.
28. Sperandio M, Pickard J, Unnikrishnan S, Acton ST, Ley K. Analysis of leukocyte rolling in vivo and in vitro. *Methods Enzymol.* 2006;416:346-371.
29. Pries AR. A versatile video image analysis system for microcirculatory research. *Int J Microcirc Clin Exp.* 1988;7(4):327-345.
30. Underhill DM, Ozinsky A. Phagocytosis of microbes: complexity in action. *Annu Rev Immunol.* 2002;20:825-852.
31. Schlumberger MC, Hardt WD. Salmonella type III secretion effectors: pulling the host cell's strings. *Curr Opin Microbiol.* 2006;9(1):46-54.

32. Kiefer F, Brumell J, Al-Alawi N, et al. The Syk protein tyrosine kinase is essential for Fcgamma receptor signaling in macrophages and neutrophils. *Mol Cell Biol.* 1998;18(7):4209-4220.
33. Weber M, Treanor B, Depoil D, et al. Phospholipase C-gamma2 and Vav cooperate within signaling microclusters to propagate B cell spreading in response to membrane-bound antigen. *J Exp Med.* 2008;205(4):853-868.
34. Luo BH, Carman CV, Springer TA. Structural basis of integrin regulation and signaling. *Annu Rev Immunol.* 2007;25:619-647.
35. Smith ML, Sperandio M, Galkina EV, Ley K. Autoperfused mouse flow chamber reveals synergistic neutrophil accumulation through P-selectin and E-selectin. *J Leukoc Biol.* 2004;76(5):985-993.
36. Zhang H, Schaff UY, Green CE, et al. Impaired integrin-dependent function in Wiskott-Aldrich syndrome protein-deficient murine and human neutrophils. *Immunity.* 2006;25(2):285-295.
37. Alon R, Dustin ML. Force as a facilitator of integrin conformational changes during leukocyte arrest on blood vessels and antigen-presenting cells. *Immunity.* 2007;26(1):17-27.
38. Smith A, Stanley P, Jones K, Svensson L, McDowall A, Hogg N. The role of the integrin LFA-1 in T-lymphocyte migration. *Immunol Rev.* 2007;218:135-146.
39. Hapfelmeier S, Hardt WD. A mouse model for *S. typhimurium*-induced enterocolitis. *Trends Microbiol.* 2005;13(10):497-503.
40. Woolf E, Grigorova I, Sagiv A, et al. Lymph node chemokines promote sustained T lymphocyte motility without triggering stable integrin adhesiveness in the absence of shear forces. *Nat Immunol.* 2007;8(10):1076-1085.
41. Cairo CW, Mirchev R, Golan DE. Cytoskeletal regulation couples LFA-1 conformational changes to receptor lateral mobility and clustering. *Immunity.* 2006;25(2):297-308.